

Synthesis, Electrochemical, Spectrophotometric and Potentiometric Studies of Two Azo-Compounds Derived from 4-Amino-2-Methylquinoline in Ethanolic-Aqueous Buffered Solutions

Mona A. El-Attar,*^a Iqbal M. Ismail^b and Mohamed M. Ghoneim^a

^aAnalytical Chemistry Research Unit, Chemistry Department, Faculty of Science, Tanta University, 31527 Tanta, Egypt

^bChemistry Department, Faculty of Science, King Abdul Aziz University, 21589 Jeddah, Saudi Arabia

Dois compostos-azo, 2-metil-4-(5-amino-2-hidróxi-fenilazo)-quinolina e 2-metil-4-(5-amino-2-hidróxi-nitrofenilazo)-quinolina, derivados da 4-amino-2-metilquinolina foram sintetizados. Suas estruturas químicas foram caracterizadas e confirmadas através de análise elementar, espectroscopia no infravermelho (IR), ressonância magnética nuclear (RMN) de ¹H e espectrometria de massas (MS). O comportamento eletroquímico do composto de partida (4-amino-2-metilquinolina) e dos dois azo-derivativos sintetizados foi estudado com um eletrodo de mercúrio em solução tampão universal B-R em diferentes valores de pH (2-11,5) contendo etanol 40% (v/v) usando polarografia dc, voltametria cíclica e coulometria com potencial controlado. Os caminhos de reação dos compostos no eletrodo foram elucidados e são discutidos. As constantes de dissociação (pK_a) dos compostos examinados, constantes de estabilidade e estequiometria dos complexos formados em soluções dos compostos com alguns íons de metais de transição (Co(II), Ni(II), Cu(II), La(III) and UO₂²⁺) foram determinadas.

Two azo-compounds, 2-methyl-4-(5-amino-2-hydroxy-phenylazo)-quinoline (**2**) and 2-methyl-4-(2-hydroxy-5-nitrophenylazo)-quinoline, derived from 4-amino-2-methylquinoline were synthesized. Their chemical structures were characterized and confirmed by means of elemental chemical analysis, infrared (IR) spectroscopy, ¹H nuclear magnetic resonance (NMR) and mass spectrometry (MS). The electrochemical behavior of the starting compound (4-amino-2-methylquinoline) and of the two synthesized azo-derivatives was studied at the mercury electrode in the B-R universal buffer at various pH values (2-11.5) containing 40% (v/v) ethanol using dc-polarography, cyclic voltammetry and controlled-potential coulometry. Their electrode reaction pathways were elucidated and discussed. The dissociation constants (pK_a) of the examined compounds, stability constants and stoichiometry of their complexes in solution with some transition metal ions (Co(II), Ni(II), Cu(II), La(III) and UO₂²⁺) were determined.

Keywords: 4-amino-2-methylquinoline, azo-derivatives, voltammetry, spectrophotometry, potentiometry

Introduction

Synthetic azo-dyes are among the most explored classes of organic compounds. Azo-dyes are widely used in many practical applications such as photochromic materials, colorants, non-linear optics, sensors and indicators.¹⁻¹² The synthesis and spectral properties of several azo-dyes as well as of their transition metal complexes have been reported in the literature.¹³⁻¹⁷ The electrochemical behavior and

electrode reaction pathways of numerous azo-dyes in various supporting electrolytes were studied and discussed.¹⁸⁻²⁵ Although the electrochemical behavior of some Schiff base compounds derived from 4-amino-2-methylquinoline has been reported,²⁶ no studies concerning the electrochemical behavior of the latter one or its azo-derivatives are reported in the literature to date.

In the present work, two azo-derivatives from 4-amino-2-methylquinoline were synthesized and characterized. Their electrochemical behavior was investigated at mercury electrodes. Besides, the dissociation constants (pK_a)

*e-mail: maema.2011@yahoo.com

of the investigated compounds, stability constant and stoichiometry of their metal complexes in solution with some transition metal ions were determined.

Experimental

Synthesis of 2-methyl-4-(5-amino-2-hydroxy-phenylazo)-quinoline (2)

According to the general procedure for synthesis of azo-compounds reported in the literature,²⁷ 0.01 mol of the starting compound, 4-amino-2-methylquinoline (1) (Aldrich), was converted to 4-(diazonium salt)-2-methylquinoline by dissolving in a mixture consisting of 4 mL water and 8 mL of 9.8 mol L⁻¹ HCl. The reaction mixture was stirred until a clear solution was obtained; cooled over crushed ice at 0-5 °C, then 5 mL water containing 0.01 mol of sodium nitrite were added portion wise under gentle stirring for 30 min to complete the reaction.²⁷ The resulting diazonium salt was slowly added under moderate stirring to a pre-cooled solution of *p*-aminophenol (Aldrich) (0.01 mol) dissolved in 30 mL of 10% (v/v) NaOH aqueous solution and stirred for 30 min, then allowed to reach room temperature. The final product was obtained as a colored azo-dye (2-methyl-4-(5-amino-2-hydroxy-phenylazo)-quinoline), which was separated, filtered and several times washed with bidistilled water, dried under vacuum and recrystallized from ethanol to give brown crystals of compound (2). Yield 67%; mp 98 °C; anal. calcd. for C₁₆H₁₄N₄O (278.12 g mol⁻¹) C, 69.05; H, 5.07; N, 20.13; found C, 69.73; H, 5.65; N, 20.52;

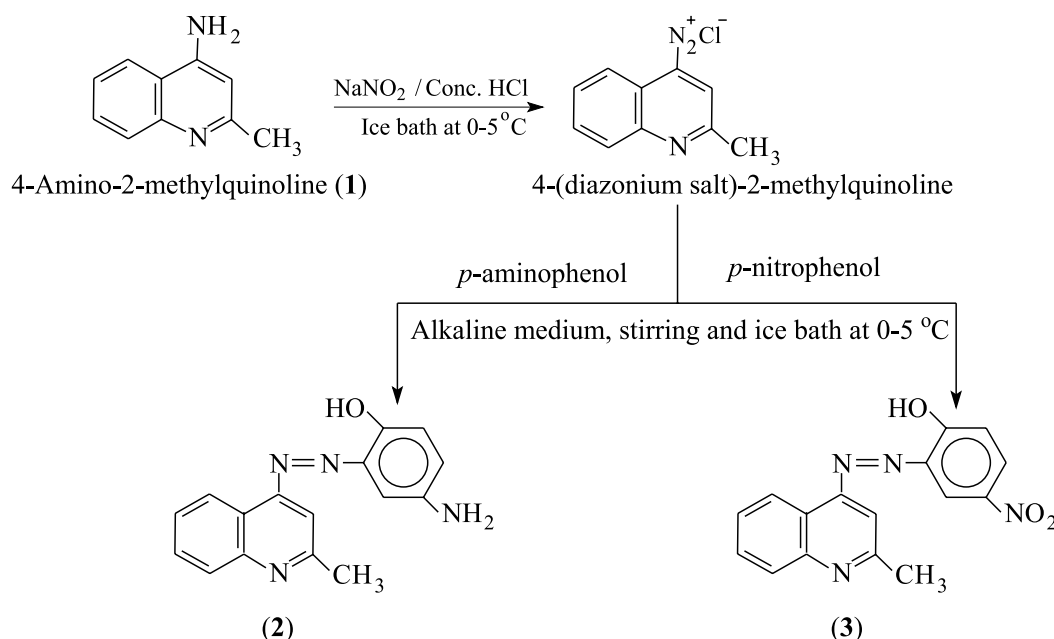
IR (KBr) ν_{\max} /cm⁻¹ 3403 (OH), 1650 (N=N), 2975 (CH₃); ¹H NMR (DMSO-*d*₆, 298 K, TMS) δ /ppm 2.41 (s, 3H, CH₃); 4.23 (s, 2H, NH₂), 5.11 (s, OH), 7.14 (s, pyridyl H), 6.55-7.32 (m, 3H subs. phenyl), 7.42-8.12 (m, 4H fused phenyl). The diazo-coupling reaction²⁷ for synthesis of compound (2) is illustrated in Scheme 1.

Synthesis of 2-methyl-4-(2-hydroxy-5-nitrophenylazo)-quinoline (3)

2-Methyl-4-(2-hydroxy-5-nitrophenylazo)-quinoline (3) was synthesized in a similar fashion as compound (2) but using *p*-nitrophenol (Aldrich) instead of *p*-aminophenol to give yellow crystals. Yield 64%; mp 112 °C; anal. calc. for C₁₆H₁₂N₄O₃ (308.09 g mol⁻¹) C, 62.33; H, 3.92; N, 18.17; found C, 62.85; H, 4.15; N, 18.64; IR (KBr) ν_{\max} /cm⁻¹ 3327 (OH), 1662 (N=N), 2948 (aliphatic H), 1390 (NO₂); ¹H NMR (DMSO-*d*₆, 298 K, TMS) δ /ppm 2.52 (s, 3H, CH₃), 6.34 (s, pyridyl H), 7.3-7.6 (m, 3H, subs. phenyl), 7.38-7.96 (m, 4H, fused phenyl). The diazocoupling reaction²⁷ for synthesis of compound (3) is illustrated in Scheme 1.

Solutions

Standard stock solutions (5 × 10⁻³ mol L⁻¹) of each of the investigated compounds (1, 2 and 3) were prepared in appropriate volume of ethanol (Merck). Desired diluted solutions were prepared by accurate dilution of the standard stock solutions with ethanol. Solutions (2 × 10⁻³ mol L⁻¹) of each of the metal salts (CoCl₂·6H₂O, NiCl₂·6H₂O, CuCl₂·2H₂O, La(NO₃)₃·6H₂O and UO₂(Ac)₂·2H₂O) were



Scheme 1. Diazo-coupling reaction for synthesis of the two azo-compounds (2 and 3).

also prepared by dissolving the accurate weight of the metal salt in appropriate volumes of deionized water. Also, 0.01 mol L⁻¹ HCl, 1 mol L⁻¹ KCl and 0.02 mol L⁻¹ NaOH solutions were prepared in deionized water.

A set of the Britton-Robinson (B-R) universal buffer of pH values 2-11.5 was prepared in bidistilled water and used as a supporting electrolyte in the presence of 40% (v/v) ethanol. All chemicals used were of analytical grade (BDH or Merck) and were used without further purification.

Apparatus and procedures

Physical measurements

Elemental analysis of the synthesized azo-compounds (**2** and **3**) was carried out using Perkin Elmer 2400 elemental analyzer (Central Laboratory for Searching & Microanalysis, Tanta University, Egypt). Their melting points were measured using a Gallenamp apparatus and were uncorrected. Infrared (IR) spectra of the solid compounds were recorded on a Jasco FT/IR-4100-A spectrophotometer within the range 4000-400 cm⁻¹ as KBr discs (Microanalytical unit, Kafr El-Sheikh University, Egypt). ¹H nuclear magnetic resonance (NMR) spectra were recorded on a Varian EM 390-90 NMR spectrometer (Micro Analysis Center, Cairo University, Egypt) using DMSO-*d*₆ (Merck) as a solvent and tetramethylsilane (TMS) as an internal standard at room temperature. The ¹H NMR chemical shifts (δ , ppm) are given relative to residual solvent peak. Mass spectral measurements of the synthesized compounds were made on a DI Analysis Shimadzu Qp-2010 Plus (Micro Analysis Center, Cairo University, Egypt).

Electrochemical measurements

A Sargent-Welch Polarograph model 4001 (Fisher, USA) was used in the dc-polarographic measurements. The electrochemical cell used was as described by Meites.²⁸ Characteristics of the capillary used as dropping mercury electrode (DME) were *m* of 1.2 mg s⁻¹ and *t* of 3.5 s in a solution of 0.1 mol L⁻¹ KCl at open circuit and a mercury height of 60 cm. A saturated calomel electrode (SCE) was used as a reference electrode.

A computer-controlled Potentiostat/Galvanostat model 273A-PAR (Princeton Applied Research, Oak Ridge, TN, USA) and the electrode assembly model 303A-PAR with the software package 270/250-PAR were used in cyclic voltammetric measurements. A micro-electrochemical cell incorporated of a three-electrode configuration system comprising of a hanging mercury drop electrode (HMDE) as a working electrode (surface area of 0.026 cm²), an Ag/AgCl/KCl_s reference electrode and a platinum wire auxiliary electrode was used.

Mercury, gold, platinum and various carbonaceous materials are the most frequently used working electrodes in electrochemical studies. The use of mercury electrodes has been recently discouraged mainly due to environmental reasons (Hg is a toxic element). Mercury has a high hydrogen overvoltage that greatly extends the cathodic potential window up to about -2 V in aqueous solution. Due to its wide cathodic potential window, mercury was frequently used as working electrodes (e.g., DME and HMDE) for electroreduction of substances of very negative reduction potential in aqueous electrolyte. Besides, it was successfully used as a working electrode for substance that strongly adsorbs onto the surface of solid electrodes. The mercury electrode is far superior to other solid electrodes in this regard since great care must be exercised with such solid electrodes to ensure that their surfaces are not changed by the electrochemical reactions. On the other side, mercury electrode (e.g., DME) also possesses a highly reproducible, readily renewable and smooth surface.

The appropriate concentration of each of the examined compounds in 10 mL B-R universal buffer in the presence of 40% (v/v) ethanol was introduced into the electrochemical cell, and then deoxygenated with pure nitrogen gas for about 10 min and for 30 s in each successive cycle, while a stream of nitrogen gas was kept over the solution during the measurements.

A potentiostat/galvanostat model 173-PAR incorporated with a digital coulometer model 179-PAR (Princeton Applied Research, Oak Ridge, TN, USA) was used for the controlled-potential coulometric measurements at a mercury pool cathode. A micro-coulometric cell incorporated with a Pt wire sealed through the cell bottom for contact with the mercury pool as a working electrode, a reference SCE and a platinum gauze as a counter electrode was used.

Controlled-potential electrolysis of solution (2.5 × 10⁻⁴ mol L⁻¹) of each of the investigated compounds was performed in the B-R universal buffer of various pH values containing 40% (v/v) ethanol to determine the total number of electrons consumed in the overall electrode reaction. The applied potential was adjusted to be around the half-wave ($E_{1/2}$) potential (± 0.1 V vs. SCE) or at the plateau of the limiting current of each of the recorded reduction waves. Prior to measurements, the electrolyzed solutions were deoxygenated by bubbling with pure nitrogen gas. During the measurements, a constant stream of nitrogen gas was passed over the surface of the electrolysis solution. The total charge *Q* (Coulombs) consumed during the complete electrolysis of the reactant was calculated by electronically integrating the current, after subtracting the background current. The number

of electrons (n) transferred *per* electrolyzed molecule at various pH values was estimated using Faraday's equation: $N = Q/nF$ where N is the number of moles of substance being electrolyzed and F the Faraday's constant ($96,485 \text{ C mol}^{-1}$).

A pH-meter model HI8014 (Hanna Instruments, Italy) accurate to ± 0.01 pH units was used for the pH measurements. A Mettler balance (Toledo-AB104, Greifensee, Switzerland) was used for weighing the solid materials. Deionized water was obtained from a Purite-Still Plus deionizer connected to an AquaMatic double-distillation water system (Hamilton Laboratory Glass Ltd., Kent, UK).

Spectrophotometric measurements

UV-Visible absorbance spectra of the examined compounds were recorded within the wavelength range 200-800 nm at room temperature using a Shimadzu UV-Vis spectrophotometer model 160A (Kyoto, Japan) with a quartz spectrometric cell (1 cm bath length). The absorbance spectra were scanned for the following mixtures: 5 mL of B-R universal buffer + 4.8 mL H_2O + 0.2 mL EtOH as blank, while for the sample 5 mL of B-R universal buffer + 4.8 mL H_2O + 0.2 mL of $2.5 \times 10^{-3} \text{ mol L}^{-1}$ azo-compound dissolved in ethanol.

Potentiometric measurements

Potentiometric measurements were performed using a pH-meter model HI8014 (Hanna Instruments, Italy) accurate to ± 0.01 pH units. The electrode was standardized before and checked after each titration with standard buffer solution (Fisher, New Jersey, USA). A standard 0.02 mol L^{-1} NaOH aqueous-ethanolic solution (40% v/v ethanol) was added from a 5 mL total volume micro burette accurate to 0.01 mL and the contents of the titration vessel were stirred using a magnetic stirrer (Sargent-Welch, USA). All titration measurements were carried out at 298 K by circulating water from an Ultra-thermostat (JULABO F10, Seelbach, Germany) through the annular space of a double-walled Pyrex titration cell of 50 mL capacity. Each of the following mixtures was prepared and potentiometrically titrated against a standard 0.02 mol L^{-1} NaOH aqueous-ethanolic solution (40% v/v ethanol) at 298 K. The volume was made up to 50 mL using bidistilled water before the titration, keeping ethanol content at 40% (v/v) in all titrated solution mixtures: (i) 5 mL of 0.01 mol L^{-1} HCl + 5 mL of 1 mol L^{-1} KCl + 20 mL EtOH + 20 mL H_2O ; (ii) 5 mL of 0.01 mol L^{-1} HCl + 5 mL of 1 mol L^{-1} KCl + 5 mL of $5 \times 10^{-3} \text{ mol L}^{-1}$ azo compound + 15 mL EtOH + 20 mL H_2O ; and (iii) 5 mL of 0.01 mol L^{-1} HCl + 5 mL of 1 mol L^{-1} KCl + 5 mL of $5 \times 10^{-3} \text{ mol L}^{-1}$ azo-compound + 5 mL of $2 \times 10^{-3} \text{ mol L}^{-1}$

metal ion (Co(II), Ni(II), Cu(II), La(III) or UO_2^{2+}) + 15 mL EtOH + 15 mL H_2O .

A constructed QuickBasic language-PC program was used in computing the data resulted from potentiometric measurements to estimate the dissociation constants (pKa) of examined azo-derivatives and the stability constants and stoichiometry of their metal-complexes in solution.

Results and Discussion

Characterization of the synthesized azo-derivatives (2 and 3)

As described in the Experimental section, the results provided by the different techniques are in good agreement with the chemical formulae proposed for the synthesized compounds **2** and **3**. IR spectra of compounds **2** and **3** are shown in the Supplementary Information (SI) section (Figure S1). In this section, the mass spectra of compounds **2** and **3** (Figure S2) and their fragmentation patterns (Figures S3 and S4) are presented. The IR spectral bands of compounds **2** and **3** at $1650\text{-}1662 \text{ cm}^{-1}$ were assigned for the N=N group. The stretching vibration bands, $\nu(\text{OH})$, of the hydroxyl group were found at $3327\text{-}3403 \text{ cm}^{-1}$. The bands at $2948\text{-}2975 \text{ cm}^{-1}$ characterize the $\nu(\text{CH}_3)$ stretching vibration. In compound **3**, the band at 1390 cm^{-1} characterizes the nitro group (Figure S1 in the SI section).

The ^1H NMR spectrum of compound (**2**) exhibited singlet for 3 protons of (CH_3) group at δ 2.41, singlet for (NH_2) at δ 4.23, singlet for (OH) at δ 5.11, singlet for pyridyl proton attached to C3 at δ 7.14, multiplet for 3 aromatic protons at δ 6.55-7.32 and multiplet for 4 protons of fused phenyl at δ 7.42-8.12.

For compound (**3**), the ^1H NMR spectrum exhibited a singlet for 3 protons of (CH_3) group at δ 2.52, singlet for pyridyl proton attached to C3 at δ 6.34, multiplet for 3 aromatic protons of substituted phenyl at δ 7.3-7.6 and multiplet for 4 protons of fused phenyl at δ 7.38-7.96.

The mass spectral assignment of compound (**2**) showed a strong molecular ion peak [M^+] at m/z (278, 48%) (Figure S2 in the SI section). Decomposition of this ion may take place through two pathways. In the first path, the compound loses CH_3 radical forming ion at m/z (263, 14%), then it loses three H radicals, producing ion with a base peak at m/z (260, 100%). The second path, [M^+] lose $\text{C}_6\text{H}_6\text{ON}$ radical, forming ion at m/z (170, 56%), this decomposition step was confirmed by the appearance of peak at m/z (108, 74%), characterized for $\text{C}_6\text{H}_6\text{ON}$ radical. The fragment ion at m/z (170, 56%) may lose nitrogen gas followed by five H radicals forming ions at m/z (142, 34%) and (137, 1%), respectively (Figure S3 in the SI section). The mass spectral assignment of compound (**3**) showed an intense

molecular ion peak $[M]^+$ at m/z (308, 100%) corresponding to the formula $C_{16}H_{12}O_3N_4$ (Figure S2 in the SI section). The $[M]^+$ may decompose through several fragmentation paths. In the first, the molecule loses $C_{10}H_8N_3$ moiety, forming ion with a peak at m/z 138, 37%. The decomposed ion ($C_{10}H_8N_3$) with peak at m/z (170, 43%) may lose CH_3 group and N_2 gas forming an ion at m/z 127, which may take hydrogen radical, forming ion with peak at m/z (128, 72%). In the second path, $[M]^+$ lose nitro group forming ion with peak at m/z (262, 59%). The third path, $[M]^+$ may lose CH_3 group and hydroxyl radical, forming ion at m/z 276, in which it takes three hydrogen radicals, forming ion with peak at m/z (279, 64%) (Figure S4 in the SI section).

Electrochemical studies

DC-polarographic and cyclic voltammetric behaviors of 4-amino-2-methylquinoline (**1**) and its two synthesized azo-derivatives (**2** and **3**) of 2.5×10^{-4} and 1×10^{-4} mol L $^{-1}$, respectively, were studied in the B-R universal buffer of various pH values (2-11.5) containing 40% (v/v) ethanol. The voltammograms of 4-amino-2-methylquinoline (**1**) exhibited a single 2-electron irreversible step in solutions of pH values (7-11) at $E_{1/2}$ ca. -1.52 to -1.71 V (Figure 1, curves a, b and c, and Figure 2, curves a and b). For 2-methyl-4-(5-amino-2-hydroxy-phenylazo)-quinoline (**2**), the voltammograms exhibited two main 2-electron irreversible cathodic steps ($E_{1/2}$ ca. -0.18 to -0.71 V and -0.75 to -1.26 V) for the 1st and 2nd waves, respectively, over the entire pH range (2-11.4) (Figure 1, curves d, e and f, and Figure 2, curves c and d). Besides, an additional irreversible cathodic step was obtained at more negative potentials ($E_{1/2}$ ca. -1.1 to -1.43 V) in solutions of pH values 4-9 (Figure 1, curve e, and Figure 2, curve c); its limiting or peak current was gradually decreased upon the increase of pH of the medium until complete disappearance at pH higher than 9 (Figure 1, curve f, and Figure 2, curve d).

For 2-methyl-4-(2-hydroxy-5-nitrophenylazo)-quinoline (**3**), the voltammograms showed a main 8-electron irreversible cathodic step ($E_{1/2}$ ca. -0.34 to -0.97 V) in solutions of pH values lower than 10 (Figure 1, 1st wave, curves g, h and i, and Figure 2, curve e), which splits into two steps in solutions of pH values higher than 10 (Figure 1, curve j, and Figure 2, curve g). An additional irreversible cathodic step was also obtained at more negative potentials ($E_{1/2}$ ca. -1.4 V) in solutions of pH values 4-9 (Figure 1, curves h and i, and Figure 2, curve f), its limiting current gradually decreased upon the increase of pH of the medium until complete disappearance at pH values higher than 9 (Figure 1, curve j, and Figure 2, curve g). The half-wave potentials ($E_{1/2}$) or the peak potentials (E_p) shifted to more

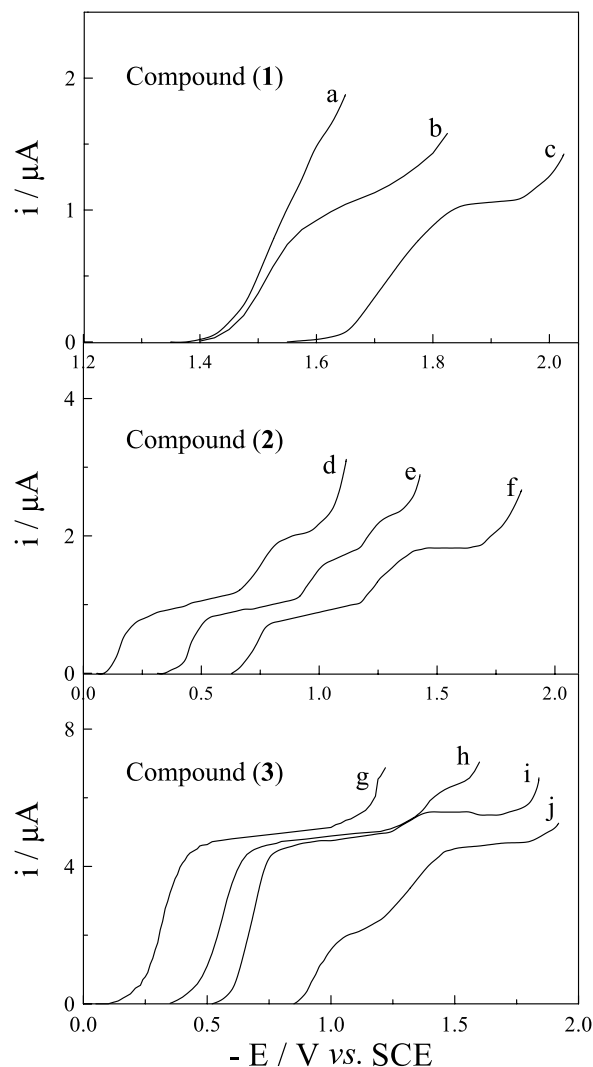


Figure 1. DC-polarograms of the examined compounds (2.5×10^{-4} mol L $^{-1}$) in the B-R universal buffer of various pH values containing 40% (v/v) ethanol, compound (**1**): (a) 6.2, (b) 7.2 and (c) 11.0, compound (**2**): (d) 2.0, (e) 7.1 and (f) 11.4, and compound (**3**): (g) 2.4, (h) 6.1, (i) 7.7 and (j) 11.4.

negative values on the increase of either the pH of the medium and the scan rate v , indicating the involvement of proton in the electrode processes²⁹ and the irreversible nature of the reduction processes,^{29,30} respectively.

The reduction waves of the examined compounds at the DME were analyzed using the fundamental equation for the irreversible polarographic waves:²⁸

$$E_{d.e.} = E_{1/2} - (0.0591/\alpha n_a) \log (i/(i_1 - i)) \quad (1)$$

Plots of $E_{d.e.}$ vs. $\log (i/(i_1 - i))$ for the polarographic waves of investigated compounds at various pH values were straight lines with slope values S_1 ($S_1, mV = 59.1/\alpha n_a$)²⁸ reported in Table 1. Values of αn_a (α is the symmetry transfer coefficient and n_a is the number of electrons involved in the rate-determining step) at various pH values

were determined from slope S_1 (Table 1). Also the $E_{1/2}$ vs. pH plots for the polarographic waves (of pH-dependent

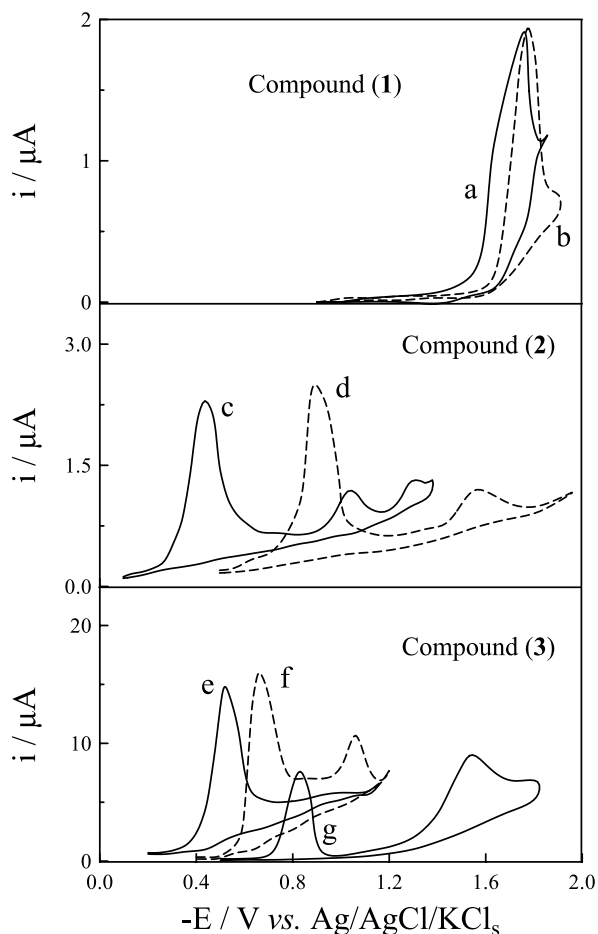


Figure 2. Cyclic voltammograms of the examined compounds (1×10^{-4} mol L^{-1}) in the B-R universal buffer of various pH values containing 40% (v/v) ethanol, compound (1): (a) 7.4 and (b) 9.2, compound (2): (c) 4.1 and (d) 11.2, and compound (3): (e) 3.3, (f) 7.4 and (g) 11.1; scan rate 500 $mV s^{-1}$.

$E_{1/2}$) of the examined compounds were straight lines with slope values S_2 reported in Table 1. The number of protons (p) participating in the rate-determining step of the reduction process of the electro-active centers of the investigated compounds was determined by applying the relationship:^{29,31}

$$\delta E_{1/2}/\delta pH = S_2 \text{ mV} = (59.1/\alpha n_a) p \quad (2)$$

$$p = S_2 (\alpha n_a/59.1) = S_2/S_1 \quad (3)$$

The data reported in Table 1 indicated that the rate-determining step of the reduction processes involved the consumption of one proton (i.e., $p = 1$) over the entire pH range. The ratio (p/n_a) may have the value 1 (when value of p and n_a are equal) or 0.5 (when value of n_a is double that of p). The most probable values obtained for α -parameter (0.40-0.55) indicated that the ratio (p/n_a) equals 0.5, which suggested that the number of electrons n_a involved in the rate-determining step of each of the electro-active centers should be double that of the involved protons (p), i.e., $n_a = 2$ and $p = 1$.

On the other side, linear E_p -pH plots of slope values (58-60 mV) at scan rate of 200 $mV s^{-1}$ for the examined compounds were obtained. From slope values (13-15 mV) of the obtained linear plots of E_p versus $\ln v$ (slope, $mV = 12.85/\alpha n_a$),³² values of αn_a (0.99-0.86) and α (0.43-0.49) were also estimated at $n_a = 2$, confirming again the irreversible nature³² of the electrode processes of the examined compounds. Moreover, values of αn_a and α were also determined at various pH values using the equation: $E_p - E_{p/2} = 0.048/\alpha n_a V$,³⁰ where ($E_p - E_{p/2}$) is the difference between cathodic peak potential E_p and the half-peak $E_{p/2}$ at half-height of peak current as a function

Table 1. Dc-polarographic data for the investigated compounds in ethanolic-aqueous B-R universal buffer solutions containing 40% (v/v) ethanol at 25 °C

pH range	S_1 / mV	αn_a	S_2 / mV	p (S_2/S_1)
Compound (1) - reduction of quinoline moiety in a single step at various pH values:				
7.0-11.0	64.5-66.7	0.91-0.88	53	0.82-0.80 p ca. 1
Compound (2) - reduction of N=N group in two steps (a) and (b), and reduction of quinoline moiety in a single step (c) at various pH values:				
2.0-11.4 (a)	68.9-69.0	0.86	56.5	0.82 p ca. 1
2.0-11.4 (b)	66.5-70.0	0.89-0.84	59.3	0.89-0.85 p ca. 1
4.0-9.0 (c)	64.4-70.3	0.92-0.84	74.9	1.16-1.07 p ca. 1
Compound (3) - reduction of both N=N azo and NO_2 groups in a single step:				
2.4-11.4	78.5-83.4	0.75-0.71	74	0.94-0.89 p ca. 1

of scan rate ν . The obtained αn_a values were found to equal (0.96-1.06) and consequently values of the symmetry transfer coefficient (α) over the pH range were found to equal (0.48-0.53) at n_a equals 2. This provided additional support of the irreversible nature³² of the electrode processes of the examined compounds.

Controlled-potential electrolysis and TLC studies

As shown in Table 2, the total number of electrons (n) transferred *per* molecule in the reduction process at various pH values for 2.5×10^{-4} mol L⁻¹ solution of each of the examined compounds (**1**, **2** and **3**) were determined by means of controlled-potential electrolysis as discussed in the Experimental section.

Table 2. Results of controlled-potential coulometry measurements for the examined compounds

Compound	pH	Number of electrons (n) transferred/molecule			
		1 st wave	2 nd wave	3 rd wave	Total
1	8.0	2	–	–	2
	11.0	2	–	–	2
2	2.8	2	2	–	4
	6.5	2	2	2	6
	11.0	2	2	–	4
3	2.4	8	–	–	8
	6.1	8	2	–	10
	11.0	4	4	–	8

Thin layer chromatographic (TLC) experiments were carried out for monitoring the products of complete electrolysis of the solution of each of the investigated azo-compounds (**2** and **3**) using benzene/acetone (70:30 v/v) as eluent. This was performed by concentration of the completely electrolyzed solution of the each of examined azo-compounds, and then followed by extraction of the buffer ingredient with ether. The TLC-experiments showed two clear spots compared to a single spot for the starting compound (**1**), indicating that two products were formed due to the reduction cleavage of the $-N=N-$ double bond. The two products were suggested to be the corresponding primary aromatic amines. The presence of the latter one was confirmed by carrying out diazo-coupling reaction^{27,33} on the completely electrolyzed solutions of each of the investigated azo-compounds. Recovery of the characteristic colored azo-dye^{27,33} in solution confirmed the presence of aromatic amines in the completely electrolyzed solution as a result of the reduction cleavage of $-N=N-$ center in each of the examined compounds (**2** and **3**), which confirmed our suggested reduction mechanisms of the investigated compounds.

On the other hand, the UV-Vis absorbance spectra of solutions (1×10^{-4} mol L⁻¹) of the investigated azo-derivatives in ethanolic-aqueous B-R universal buffer (e.g., pH 7) before controlled potential electrolysis showed a characteristic band at λ_{\max} 400 nm due to the $n-\pi^*$ transition of $-N=N-$ group (e.g., Figure 3; spectrum (a) for compound **3**). This band disappeared completely after controlled-potential electrolysis of the examined solutions (e.g., Figure 3; spectrum (b) for compound **3**). It is important to notice that the spectra of solutions of both derivatives (**2** and **3**) after controlled-potential electrolysis resemble that of the starting compound (**1**) (Figure 3; spectrum c). This behavior confirmed the cleavage of the $-N=N-$ bond in both derivatives by controlled-potential electrolysis.

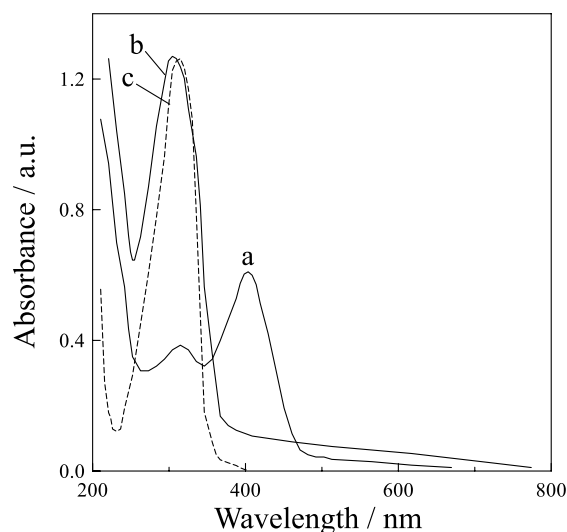


Figure 3. UV-Vis spectra of the azo-compound (**3**) (1×10^{-4} mol L⁻¹) in ethanolic-aqueous B-R universal buffer solution of pH 7: (a) before electrolysis and (b) after complete electrolysis at controlled-potential, compared to that of 1×10^{-4} mol L⁻¹ solution of the starting compound (**1**) (c).

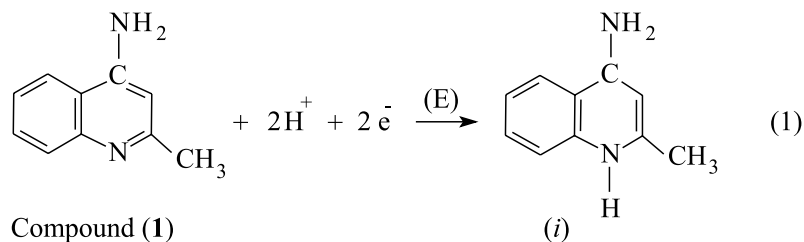
Electrode reaction pathways

Electrode reaction of compound (**1**)

4-Amino-2-methylquinoline (**1**) was reduced at the mercury electrode in buffered solutions of pH values 7-11 in a single 2-electron irreversible step which is assigned to the reduction-saturation of the $-C=N-$ double bond of its quinoline moiety,³⁴ as illustrated in Scheme 2.

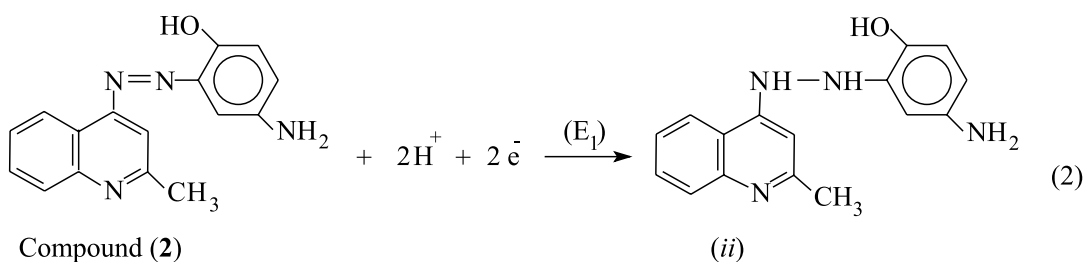
Electrode reaction of the azo-derivative (**2**)

The synthesized 2-methyl-4-(5-amino-2-hydroxy-phenylazo)-quinoline (**2**) was reduced at the mercury electrode in buffered solution of pH 2-11.5 in two 2-electron steps (1st and 2nd steps), which were attributed to the reduction of the $-N=N-$ double bond to the amine stage as illustrated in Scheme 3. The 3rd reduction step that appeared

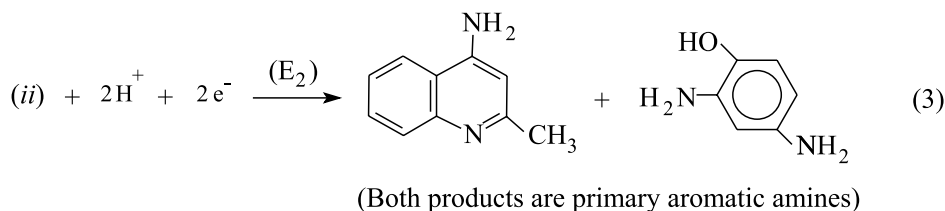


Scheme 2. Electrode reaction pathway of the parent compound (1).

First step:



Second step:



$E_1 \neq E_2$

Scheme 3. Electrode reaction pathway of the azo-derivative (2).

at more negative potential in solutions of pH values 4-9 is due to reduction of the $-C=N-$ double bond of the quinoline moiety,³⁴ as illustrated in Scheme 2 of the electrode reaction of the starting compound (1).

Electrode reaction of azo-derivative (3)

The synthesized 2-methyl-4-(2-hydroxy-5-nitrophenylazo)-quinoline (3) was also reduced at the mercury electrode in buffered solution of pH values 2-10 in a single 8-electron step, which is attributed to reduction of either the $-N=N-$ double bond to the amine stage and the $-NO_2$ group to the hydroxylamine stage, via the consumption of four electrons for each centre,^{24,35} (Scheme 4, reaction 4). At pH values higher than 10, this reduction step splits into two steps. The 1st and 2nd steps were attributed to the reduction-cleavage of the $-N=N-$ double bond to the amine stage and reduction of the NO_2 group to the hydroxylamine stage,³⁵ respectively, via the consumption of four electrons for each center (Scheme 4, reactions 5 and 6, respectively).

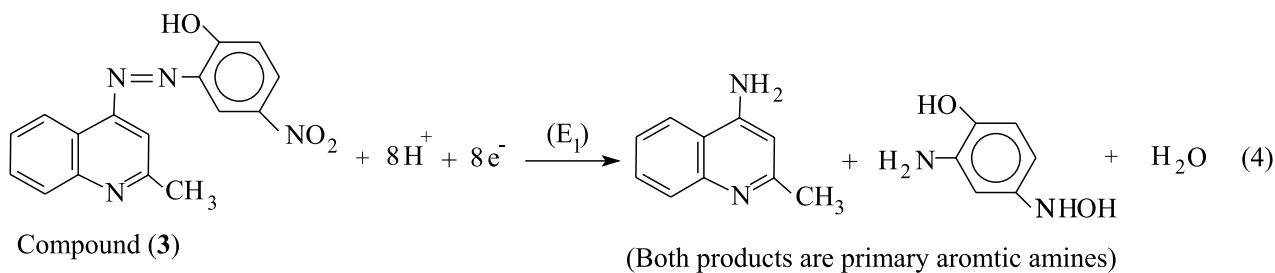
The reduction step that appeared at more negative potential in solutions of pH values 4-9 is due to reduction of the $-C=N-$ double bond of the quinoline moiety³⁴ as illustrated in Scheme 2 of the electrode reaction of the starting compound (1).

Spectrophotometric studies

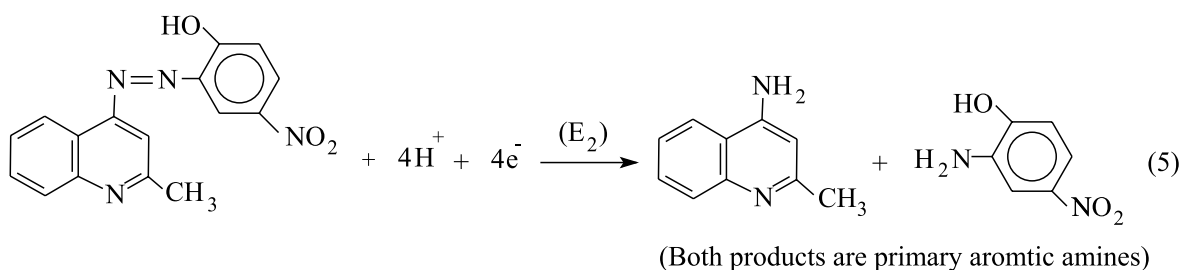
UV-Vis absorption spectra of $5 \times 10^{-5} \text{ mol L}^{-1}$ of each of compounds (2) and (3) were recorded in the B-R universal buffer of various pH values (2-12) within the wavelength range 200-800 nm. Compound 2 showed two absorption bands at λ_{max} 438 and 480 nm ($n-\pi^*$), with an isosbestic point at λ_{max} 462 nm (Figure 4). While compound 3 showed two absorption bands at λ_{max} 315 and 400 nm ($n-\pi^*$), with an isosbestic point at λ_{max} 345 nm (Figure 4).

The first band may be attributed to the non-ionized form, whereas the second one that develops as the pH increases is due to the ionized species of each of the examined

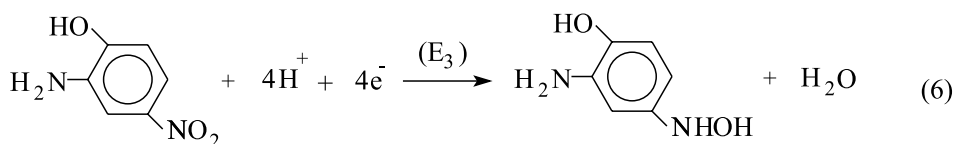
Single step (pH 2-10):



First step (pH > 10):



Second step (pH > 10):



Scheme 4. Electrode reaction pathway of azo-derivative (3).

compounds as a result of proton dissociation of the hydroxyl group. The isobestic point indicated the presence of an acid-base equilibrium between non-ionized and ionized species. The ionic form absorbs at longer wavelength indicating that the intermolecular charge transfer is easier in the ionic form than in the non-ionic one, confirming that the intermolecular charge transfer is influenced by the OH group. For 4-amino-2-methylquinoline (**1**), its absorbance spectra was also recorded under the same experimental conditions and was found to exhibit absorption band at λ_{\max} 330 nm at pH values lower than 8, whereas, at higher pH values, this band was blue shifted to λ_{\max} 300 nm. This behavior may be due to that protonation of species takes place on the nitrogen of quinoline moiety in solutions of pH lower than 8. However, with the increase of the pH values of the medium, deprotonation takes place. The changes in the absorption spectra on varying the pH of solutions were used for determination of the dissociation constant (pKa) of the examined compounds (**1**, **2** and **3**). The absorbance-

pH curves at two different wavelengths were typical Z or S-shaped (Figure 5) which indicated the transformation of the molecule from one form into another one.

Values of the dissociation constant (pKa) of the investigated compounds were determined at two different wavelengths (except compound **1**) using different methods namely: (i) half-height, (ii) limiting absorbance, (iii) modified limiting absorbance, (iv) isobestic point and (v) modified isobestic point.³⁶⁻³⁸ The obtained pKa values are reported in Table 3.

The observed high values of pKa of the synthesized azo-derivatives (**2** and **3**) may be attributed to the location of the ionizable group (-OH) in an ortho-position where it has lower ability to release H⁺ ion.^{39,40}

Potentiometric studies

The average number of protons associated with the reagent molecule \bar{n}_A at different pH values⁴¹ was calculated

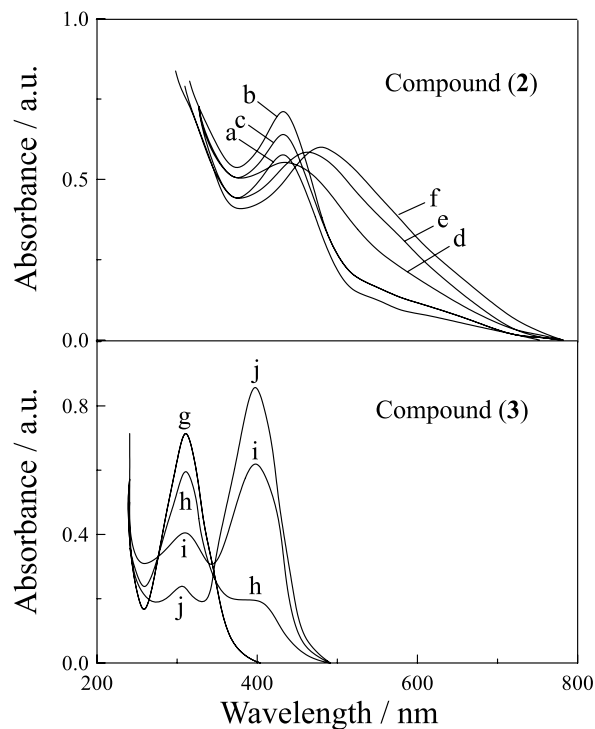


Figure 4. UV-Vis spectra of the examined compounds (5×10^{-4} mol L $^{-1}$) in B-R universal buffer of various pH values, compound (2): (a) 2, (b) 4, (c) 6, (d) 9, (e) 10 and (f) 11, and compound (3): (g) 3.0, (h) 6.3, (i) 7.3 and (j) 9.2.

from the titration curves of HCl solution in the absence and in presence of the examined azo-derivative (2 or 3) against 0.02 mol L $^{-1}$ NaOH aqueous-ethanolic solution (40% v/v ethanol) at 298 K (Figure 6). Thus, the formation curves (\bar{n}_A vs. pH) for the proton-ligand systems⁴² were constructed and found to extend between 0 and 1.0 in the \bar{n}_A scale for both compounds (2 and 3). This means that each of the examined compounds 2 and 3 has one dissociable proton from the enolized hydrogen ion of the hydroxyl group (Table 4). This indicates that the acid-base equilibrium based on the molecular form HL is in complete accordance with the following equilibrium:

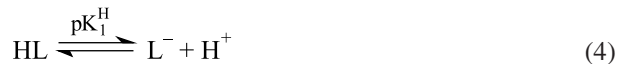


Table 3. Dissociation constants (pKa) of the compounds under investigation in ethanolic-aqueous B-R universal buffer using: the half-height (i), limiting-absorbance (ii), modified limiting-absorbance (iii), isosbestic point (iv) and modified isosbestic point (v) methods

Compound	$\lambda_{\text{max}} / \text{nm}$ ($n-\pi^*$)	Dissociation constants (pKa)					Mean value
		(i)	(ii)	(iii)	(iv)	(v)	
1	330	9.8	10.1	9.75	–	–	9.88
2	438	9.4	11.05	9.35	9.55	8.30	9.53
	480	8.6	6.35	8.40	–	–	7.78
3	315	7.4	8.20	7.35	7.25	7.05	7.45
	400	6.9	6.95	7.00	–	–	6.95

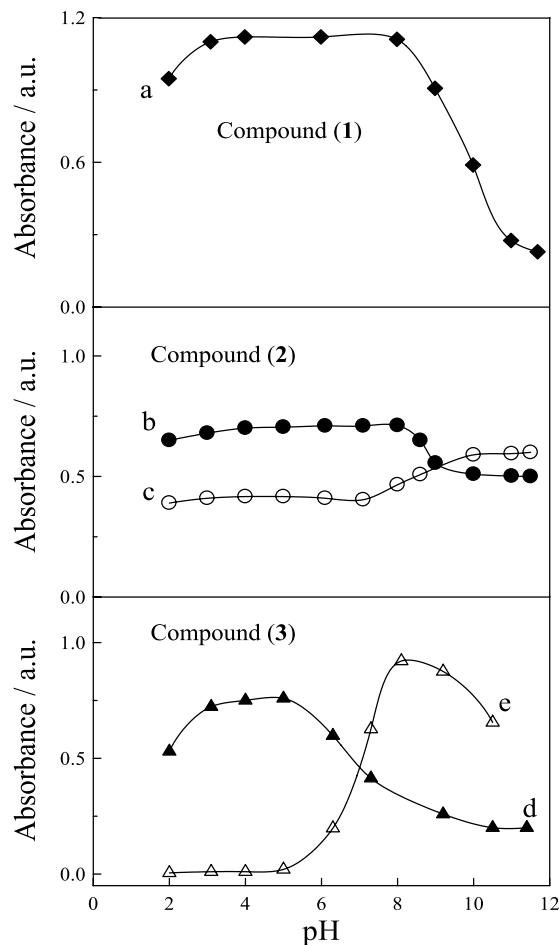


Figure 5. Plots of absorbance vs. pH of the investigated compounds (5×10^{-4} mol L $^{-1}$) in B-R universal buffer of different pH values, compound (1): λ_{max} at 330 nm (a), compound (2): λ_{max} at 438 nm (b) and 480 nm (c), and compound (3): λ_{max} at 315 nm (d) and 400 nm (e).

As shown in Table 4, compound (2) has a lower acidic character ($\text{pK}_1^{\text{H}} = 8.75$) than compound (3) ($\text{pK}_1^{\text{H}} = 7.5$). This is quite reasonable because the presence of NH_2 group enhances the electron density by its high electron-donating mesomeric and inductive effects, respectively; thereby stronger O–H bond is formed. The presence of electron-withdrawing group NO_2 leads to the opposite effect,^{39,40} thus the pK_1^{H} values for the examined compounds follow

Table 4. Stepwise stability constants (ML and ML₂ chelates) of the synthesized azo-derivatives (**2** and **3**) in 40% (v/v) ethanol-water solution containing 1 mol L⁻¹ KCl at 298 K

M ^{an}	Compound (2)			Compound (3)		
	pK ₁ ^H	log K ₁	log K ₂	pK ₁ ^H	log K ₁	log K ₂
H ⁺	8.75 ± 0.09			7.5 ± 0.1		
Co ²⁺		5.87 ± 0.07	4.02 ± 0.06		6.32 ± 0.06	5.11 ± 0.08
Ni ²⁺		6.15 ± 0.07	4.29 ± 0.09		6.95 ± 0.10	5.83 ± 0.12
Cu ²⁺		6.48 ± 0.06	4.55 ± 0.08		8.45 ± 0.11	6.30 ± 0.07
La ³⁺		6.30 ± 0.10	4.43 ± 0.09		7.54 ± 0.08	6.10 ± 0.09
UO ₂ ²⁺		6.62 ± 0.09	4.75 ± 0.10		9.26 ± 0.08	6.80 ± 0.10

Each value is the mean of three readings ± standard deviation.

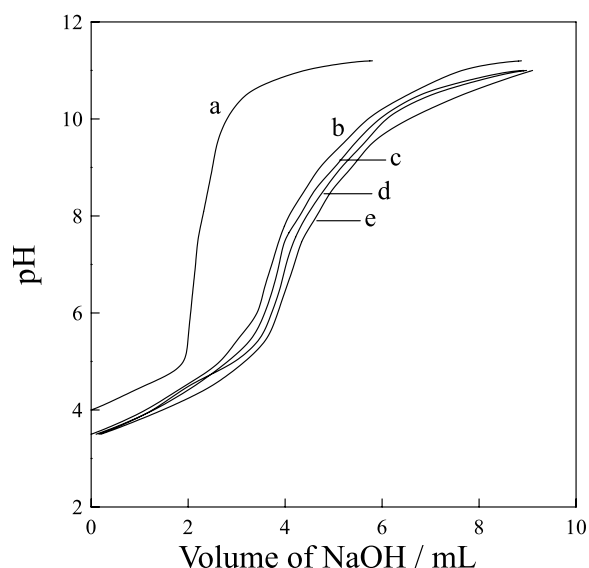


Figure 6. Potentiometric titration curves against 0.02 mol L⁻¹ NaOH ethanolic-aqueous 40% (v/v) solution at 298 K for the solution mixtures: (a) 5 mL of 0.01 mol L⁻¹ HCl + 5 mL of 1 mol L⁻¹ KCl + 20 mL EtOH + 20 mL H₂O, (b) 5 mL of 0.01 mol L⁻¹ HCl + 5 mL of 1 mol L⁻¹ KCl + 5 mL of 5 × 10⁻³ mol L⁻¹ azo-derivative (**2**) + 15 mL EtOH + 20 mL H₂O, (c) 5 mL of 0.01 mol L⁻¹ HCl + 5 mL of 1 mol L⁻¹ KCl + 5 mL of 5 × 10⁻³ mol L⁻¹ azo-derivative (**2**) + 5 mL of 2 × 10⁻³ mol L⁻¹ Co(II) + 15 mL EtOH + 15 mL H₂O, (d) the same solution mixture + 2 × 10⁻³ mol L⁻¹ Ni(II), and (e) the same solution mixture + 2 × 10⁻³ mol L⁻¹ Cu(II).

the sequence **2** > **3**. The results obtained are of the same order when compared to those spectrophotometrically obtained (Table 3).

The average number of reagent molecules attached *per* metal ion \bar{n} , at different pH values, was calculated from the titration curves of HCl solutions in the absence and the presence of the examined azo-derivative (**2** or **3**) and the selected metal ions (Co(II), Ni(II), Cu(II), La(III) or UO₂²⁺) against 0.02 mol L⁻¹ NaOH aqueous-ethanolic solution (40% v/v ethanol) at 298 K (Figure 6).

The metal-titration curves (curves c-e) were well separated from that of free ligand (curve b), along the axis of added volume of NaOH solution, which is attributed to the release of H⁺ ions as a result of the complexation process (Figure 6). The formation curves for the metal

complexes of the two azo-derivative (**2** and **3**) with the selected metal ions (Co(II), Ni(II), Cu(II), La(III) or UO₂²⁺) were obtained by plotting the average number of ligands attached *per* metal ion (\bar{n}) vs. the free ligand exponent (pL).⁴²

By analysis of the formation curves,^{43,44} the successive stability constant log K₁ and log K₂ of the studied metal complexes ML and ML₂, respectively, were determined (Table 4) using a constructed QuickBasic language-PC program. As shown in Table 4, the differences observed in the standard deviations (SD) of the obtained data under the same experimental conditions were insignificant, confirming reproducibility and precision of the results. The data obtained can be pointed out based on the following: (i) no precipitate was observed in the titration vessel, indicating that the formation of metal hydroxide is excluded; (ii) the maximum \bar{n} values for all investigated metal complexes were found to be ca. 2, revealing that both ML and ML₂ types of complexes are formed in solution; (iii) for all complexes formed log K₁ were always found higher than those of log K₂ (Table 4), because the vacant sites of the metal ions more freely available for binding of a first ligand than for a second one;^{40,45} (iv) the order of stability constants of the metal complexes of the azo-compounds (**2** and **3**) at 298 K were found as: UO₂²⁺ > La(III) < Cu(II) > Ni(II) > Co(II). The sequence of stability of complexes of compounds (**2**) and (**3**) with Cu(II) > Ni(II) > Co(II) are in agreement with that reported by Irving and Williams.^{46,47} The UO₂²⁺ has higher stability than those of the other metal complexes. This may be attributed to the bonded oxygen atoms which increase the electrostatic attraction between the metal ion and the coordinated ligands and overcome any steric hindrance offered by the oxygen of the oxygenated cations.⁴⁰

Conclusions

Two azo-compounds (2-methyl-4-(5-amino-2-hydroxy-phenylazo)-quinoline (**2**) and 2-methyl-4-(2-hydroxy-5-

nitrophenylazo)-quinoline (**3**) derived from 4-amino-2-methylquinoline (**1**) were synthesized and their chemical structures confirmed by various techniques. Their electrode reaction pathways at the DME and HMDE electrodes in buffered solutions of pH values (2-11.5) were elucidated. The dissociation constants (pKa) of the investigated compounds were determined using spectrophotometric and potentiometric methods. Besides, stability constant and stoichiometry of their metal complexes in solution with some transition metal ions (Co(II), Ni(II), Cu(II), La(III) and UO_2^{2+}) were determined potentiometrically. The results indicated the existence of ML and ML_2 types of complexes in solution.

Supplementary Information

Supplementary data of IR, and MS spectra of the two synthesized azo-compounds (2-methyl-4-(5-amino-2-hydroxy-phenylazo)-quinoline (**2**) and 2-methyl-4-(2-hydroxy-5-nitrophenylazo)-quinoline (**3**)) (Figures S1-S4) are available free of charge at <http://jbcs.sbq.org.br> as PDF file.

References

- Raposo, M. M.; Fonseca, A. C.; Castro, M. R.; Belsley, M.; Cardoso, M. S.; Carvalho, L. M.; Coelho, P. J.; *Dyes Pigm.* **2011**, *91*, 62.
- LiHong, N.; Cheng, Z.; Zihui, C.; Zhi, Z.; Zhong, Yu, L.; FuShi, Z.; YingWu, T.; *Chin. Sci. Bull.* **2009**, *54*, 1169.
- Sacarescu, L.; Sacarescu, G.; Simionescu, M.; Hurduc, N.; *J. Inorg. Organomet. Polym.* **2009**, *19*, 348.
- Dixit, B. C.; Patel, H. M.; Desai, D. J.; *J. Serb. Chem. Soc.* **2007**, *72*, 119.
- Khosravi, A.; Moradian, S.; Gharanjig, K.; Taromi, F. A.; *Iran. Polym. J.* **2005**, *14*, 667.
- Raposo, M. M.; Castro, M. R.; Fonseca, A. C.; Schellenberg, P.; Belsley, M.; *Tetrahedron* **2011**, *67*, 5198.
- Raposo, M. M.; Castro, M. R.; Belsley, M.; Fonseca, A. C.; *Dyes Pigm.* **2011**, *91*, 454.
- He, T. C.; Wang, C. S.; Pan, X.; Zhang, C. Z.; Lu, G. Y.; *Appl. Phys. B: Lasers Opt.* **2009**, *94*, 653.
- Maruo, Y. Y.; Akaoka, K.; Nakamura, J.; *Sens. Actuators, B* **2010**, *143*, 487.
- El-Safy, S. A.; *Adsorption* **2009**, *15*, 227.
- Sharma, A. K.; Singh, I.; *Food Anal. Methods* **2009**, *2*, 221.
- Sheremetev, S. V.; Kuznetsov, V. V.; *J. Anal. Chem.* **2007**, *62*, 319.
- Li, X.; Wu, Y.; Gu, D.; Gan, F.; *Dyes Pigm.* **2010**, *86*, 182.
- Sujamol, M. S.; Athira C. J.; Sindhu, Y.; Mohanan, K.; *Spectrochim. Acta, Part A* **2010**, *75*, 106.
- Nejati, K.; Rezvani, Z.; Seyedahmadian, M.; *Dyes Pigm.* **2009**, *83*, 304.
- Ahn, S. B.; Kim, J. P.; Shim, W. S.; *Fibers Polym.* **2009**, *10*, 643.
- Albayrak, C.; Gümrükçüoğlu, I. E.; Odabasoglu, M.; Iskeleli, N. O.; Agar, E.; *J. Mol. Struct.* **2009**, *932*, 4354.
- Byabartta, P.; *Russ. J. Coord. Chem.* **2009**, *35*, 687.
- Ghoneim, M. M.; El-Desoky, H. S.; Amer, S. A.; Rizk, H. F.; Habazy, A. D.; *Dyes Pigm.* **2008**, *77*, 493.
- Chandra, U.; Gilbert, O.; Swamy, B. E. K.; Bodke, Y. D.; Sherigara, B. S.; *Int. J. Electrochem. Sci.* **2008**, *3*, 1044.
- Menek, N.; Karaman, Y.; *Dyes Pigm.* **2006**, *68*, 101.
- Menek, N.; Karaman, Y.; *Dyes Pigm.* **2005**, *67*, 9.
- Menek, N.; Basaran, S.; Turgut, G.; Odabasoglu, M.; *Dyes Pigm.* **2004**, *61*, 85.
- La-Scalea, M. A.; Serrano, S. H. P.; Gutz, I. G. R.; *J. Braz. Chem. Soc.* **1999**, *10*, 127.
- Goyal, R. N.; Verma, M. S.; Singhal, N. K.; *Croat. Chem. Acta* **1998**, *71*, 715.
- Moharram, Y. I.; El-Hallag, I. S.; El-Attar, M. A.; Ghoneim, M. M.; *Bull. Electrochem.* **2005**, *21*, 297.
- Vogel, A. I.; *A Text Book of Practical Organic Chemistry*, 3rd ed.; Longman Publishers: New York, 1961.
- Meites, L.; *Polarographic Techniques*, 2nd ed.; Interscience Publishers: New York, 1965, p. 232-248.
- Zuman, P.; *The Elucidation of organic Electrode Process*; Academic Press: New York, 1969. p. 22-24.
- Greef, R.; Peat, R.; Peter, L. M.; Pletcher, D.; Robinson, J.; *Instrumental Methods in Electrochemistry, Southampton Electrochemistry Group*; Ellis Horwood Limited, John Wiley & Sons: New York, 1985, p. 187.
- Ghoneim, M. M.; Ashy, M. A. A.; *Can. J. Chem.* **1979**, *57*, 1249.
- Galus, Z.; *Fundamentals of Electrochemical Analysis*; John Wiley: New York, 1976, p. 238.
- Pavia, D. L.; Lampman, G. M.; Kriz, G. S.; Engel, R. G.; *Introduction to Organic Laboratory Techniques - Small-Scale Approach*, 1st ed.; Harcourt Brace: Florida, 1998, p. 313-322.
- Stradyn, Y. P.; Kadysh, V. P.; Giller, S. A. I.; *Khim. Geterotsikl. Soedin.* **1973**, *12*, 1587.
- Zuman, P.; *Microchem. J.* **1997**, *57*, 4-51.
- Issa, R. M.; El-Ezaby, M. S.; Zewail, A. H.; *Z. Phys. Chem. (Leipzig)* **1970**, *244*, 155.
- Issa, I. M.; Issa, R. M.; El-Ezabey, M. S.; Ahmed, Y. Z.; *Z. Phys. Chem. (Leipzig)* **1969**, *242*, 169.
- Abdelhal, F. M.; Issa, R. M.; El-Ezabey, M. S.; Hasanein, A. A.; *Z. Phys. Chem. (Frankfurt)* **1970**, *73*, 59.
- McMurry, J.; *Organic Chemistry*, 5th ed.; Brooks/Cole: USA, 2000.
- Shehatta, I.; Kenawy, I.; Askalany, A. H.; Hassan, A. A.; *Can. J. Chem.* **2001**, *79*, 42.

41. Fronaeus, S.; *Complex System of Copper*; Gleer Upska Universitets-Bokhandeln: Lund, 1948.
42. Irving, H. M.; Rossotti H. S.; *J. Chem. Soc.* **1954**, 76, 2904.
43. Rossotti, F. J. C.; Rossotti, H. S.; *Acta Chem. Scand.* **1955**, 9, 1166.
44. Beck, M. T.; Nagybal, I.; *Chemistry of Complex Equilibria*; Wiley: New York, 1990.
45. Ghoneim, M. M.; El-Hallag, I. S.; El-Baradie, K. Y.; El-Desoky, H. S.; El-Attar, M. A.; *Monatsh. Chem.* **2006**, 137, 285.
46. Irving, H. M.; Williams, R. J. P.; *Nature* **1948**, 162, 746.
47. Irving, H. M.; Williams, R. J. P.; *Analyst* **1952**, 77, 813.

Submitted: April 3, 2012

Published online: July 31, 2012